

Modelling of regenerative braking

Valentin Totev ¹, Vultchan Gueorgiev ²

Faculty of Electrical Engineering

Technical University - Sofia

Sofia, Bulgaria

valentintotev@tu-sofia.bg ¹, vulchy@tu-sofia.bg ²

Abstract— This paper presents a discussion about simulation modelling of regenerative braking of electric vehicles. Electric vehicles are widely topical. Their drivetrain system can be effectively presented by an equivalent system consisting of a battery, a motor and a power converter. Regenerative braking enables part of energy used for braking to be transformed as electrical and recaptured by charging the battery. As this is one of the main advantages of these vehicles over petrol ones, this paper is purposed to explore the modelling and simulation of regenerative braking in MATLAB/ Simulink environment. The model is considered for said equivalent system and consists of a Li-ion battery, a permanent magnet synchronous motor and a power converter. Results from simulation display a satisfactory torque and currents response as well as a raise in state-of-charge of the battery during regenerative periods with negative torque values. Following the simulation results a brief description of a stand for physical modelling of regenerative braking and studying in laboratory environment is given.

Keywords—electric vehicles, regenerative braking,

I. INTRODUCTION

Awareness of necessity and need for cleaner energy utilization in order to preserve the environment has risen over the years. Part of this looming threat for the environment lies within fossil fuelled vehicles with internal combustion engines (ICE's). Thus, electric vehicles (EV's) have become more topical as a mean of transportation with reduced in hybrids and plug-in hybrids (HEV and PHEV) or even without emissions in full electric or battery EV's (BEV). While an electrical drivetrain, driven by an electric motor, has numerous advantages over its equivalent ICE powertrain, it seems as though it is still widely emphasized on EV's disadvantages. Primarily, mass attention is focused on their shorter driving range per charge of their batteries. However, EV's can perform regenerative braking. Regenerative braking in essence allows part of energy used for braking to be restored back to its batteries and to be further utilized again. Thus EV's energy expenses can be reduced and driving range can be increased. While the problem with development of an appropriate charging infrastructure accordingly with each power system is still very much far from being answered on a global scale, regenerative braking will contribute a significant part to EV's future success.

II. ELECTRIC VEHICLE'S MOTOR

Generally, EV's are driven by a permanent magnet synchronous motor (PMSM). These motors are characterized by higher power density, higher reliability, better efficiency, better mechanical characteristics, higher torque, lower noise during operation, better heat dissipation, being smaller in size, lower losses due to rotor's construction, etc. when compared to other types of electric motors [1] – [3].

Drawbacks of a PMSM include high cost of permanent magnets, presence of cogging torque, presence of reluctance torque in salient pole PMSM's, etc. Cogging torque is caused by the interaction between permanent magnets in the rotor and stator's teeth [4], [5].

Permanent magnet machines can be conditionally classified in three ways. Firstly, based on the direction of field's flux they can be classified as ones with radial or with axial field [4].

Secondly, in terms of magnet placement on the rotor they can be classified as Surface PMSM's (SPMSM) and Interior PMSM's (IPMSM). The method used for mounting permanent magnets on the rotor determines a difference in inductances along the direct and quadrature axes – L_d and L_q respectively, i.e. whether the machine is salient poled [4].

Permanent magnets in SPMSM are placed on the circumference of the rotor. These motors are characterized by higher air gap flux, but are not suited for high velocity operations. They also have lower robustness than interior ones. For SPMSM's it can be considered that inductances L_d and L_q are equal (non-salient pole) [4], [5].

IPMSM's have their magnets embedded in their rotor. They are more robust than SPMSM's and are appropriate for high velocity applications. The ratio between inductances is in the range of $L_q/L_d > 3$ (salient pole) [1], [4].

Thirdly, in terms in terms of operation these machines can be classified as PMSM and brushless dc (BLDC). Both types are typically controlled by field-oriented control (FOC) but with different switching algorithms. PMSM's are controlled by pulse-width modulation (PWM) and induced EMF has sinusoidal waveform. On the other hand, BLDC's are controlled by six-step switching where at any given point of time only two phases are conducting and induced EMF has trapezoidal shaped waveform.

A. Mathematical description of a Permanent Magnet Synchronous Motor

A description of a PMSM's quantities in rotor reference frame referred to the stator is presented by (1) – (4) [4], [6], [7].

$$\frac{d}{dt} i_d = \frac{1}{L_d} v_d - \frac{R}{L_d} i_d + \frac{L_q p}{L_d^2} \omega_m i_q \quad (1)$$

$$\frac{d}{dt} i_q = \frac{1}{L_q} v_q - \frac{R}{L_q} i_q - \frac{L_d p}{L_d^2} \omega_m i_d - \frac{\lambda_p^2 \omega_m}{L_q} \quad (2)$$

where i is current, v is voltage, R is resistance of stator's coil, L is inductance, $p/2$ is number of pole pairs, λ is flux linkage of permanent magnets, ω_m is rotor's angular velocity. Indices d and q denote respective axis.

Electromagnetic torque can be expressed by:

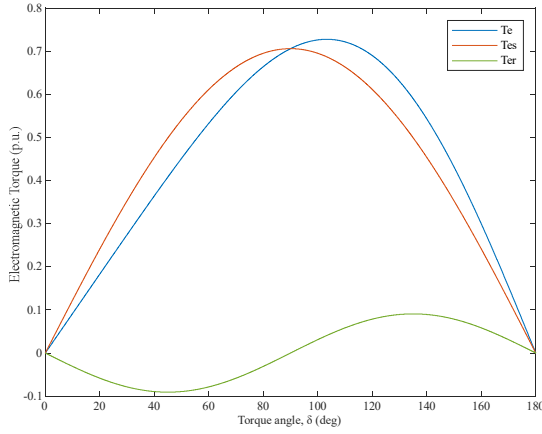


Fig. 1. Effect of reluctance torque on electromagnetic torque.

$$T_e = \frac{3p}{2} [\lambda i_q + (L_d - L_q) i_d i_q] \quad (3)$$

When $L_d = L_q$, as for a surface PMSM (SPMSM) or whenever controlling by $i_d = 0$, then (3) becomes as:

$$T_e = \frac{3p}{2} \lambda i_q \quad (4)$$

Angular velocity is obtained from equation of motion:

$$\frac{d}{dt} \omega_m = \frac{1}{J} (T_e - T_f - F \omega_m - T_m) \quad (5)$$

$$\frac{d}{dt} \theta_m = \omega_m \quad (6)$$

where T_f is static friction torque on the shaft, F is viscous friction, T_m is mechanical torque on the shaft, θ_m is rotor's angular position.

If a salient pole PMSM is considered (IPMSM) and stator current components i_q and i_d are expressed as [4]:

$$i_q = I_m \sin \delta \quad (7)$$

$$i_d = I_m \cos \delta \quad (8)$$

where I_m is peak value of stator's current vector and δ is torque angle. This is the angle between stator's current vector and rotor's flux vector [1], [4].

Two torque components dependent on torque angle stand out clearly in (3). The first component T_{e_s} (9) is synchronous torque, caused by permanent magnet's flux. The other component T_{e_r} (10) is reluctance torque, caused by different reluctances on d and q axes [1], [4], [6].

$$T_{e_s} = \frac{3p}{2} \lambda I_m \sin \delta \quad (9)$$

$$T_{e_r} = \frac{3p}{2} \left[\frac{1}{2} (L_d - L_q) \right] I_m^2 \sin 2\delta \quad (10)$$

Fig. 1 presents an example of relations of said torques to torque angle and the effect of reluctance torque. As it can be seen, the maximum value of total electromagnetic torque T_e occurs at a torque angle of about 105 to 110 ° due to the presence of reluctance torque.

B. Control of a Permanent Magnet Synchronous Motor

Generally, PMSM's are controlled by FOC. Angular position of rotor is a significant parameter in FOC. BLDC's rotor position typically can be determined by signals of three Hall sensors, while PMSM's can use either a Hall sensor, or a quadrature encoder [3], [8].

Throughout the years sensorless FOC has become more widely used than sensor based [5], [9]. Disadvantages of sensor based control include lower reliability as more components are introduced and additional cost for each one of them. Information about rotor's angular position is essential in FOC. Sensorless based FOC estimates rotor's position by measurements of speed, voltages and currents.

Space vector pulse – width modulation (SVPWM) is one of the most widely applied algorithm with FOC [3], [5], [9]. SVPWM is characterized with lower switching losses, lower harmonics and has higher utilization of voltage compared to sinusoidal PWM (SPWM) [3].

III. REGENERATIVE BRAKING AND MODELLING OF REGENERATIVE BRAKING

Regenerative braking is one of the main advantages of EV's. It is purposed to reduce emissions in HEV and PHEV as well as to increase driving range in BEV. The effect of regenerative braking can be especially noticed in urban driving where lots of stop-and-go driving occurs. One of the most common strategies to govern regenerative braking is short circuit braking [10], [11]. This strategy consists of control of only lower side switches of power converter. Fig. 2 shows a visualization of the following explanation. Two periods of control can be observed. In first period, termed coasting, there is a short circuit between motor's phases and battery is not being charged. This is done for a very brief period of time which suggests that it is not the case of short circuit fault. In this way connecting PMSM's phases with each other creates an equivalent circuit of a boost converter. In second period circuit closes through upper side back diodes and battery is being charged. Thus, the method of short circuit braking can be utilized to increase PMSM's output voltage when operating as generator without additional external components.

Modelling of regenerative braking considered in EV's is done in MATLAB/Simulink environment with Simscape library. A Simulink model of the system is presented on Fig. 3. The model consists of a lithium- ion (Li- ion) battery, a three- phase power converter, a PMSM, control subsystem and measurements of various quantities.

In the model a three- phase power converter with MOSFET's is considered. Power converter's gate signals are produced by Control subsystem based on motor's speed and a speed reference. Details of PMSM, battery and control subsystem are given in following subsections.

While the vehicle's geometrical parameters, curb mass, slip between tire and road, and blending between mechanical braking system and regenerative braking, the considered approach is primarily focused from electrical standpoint to explore the efficiency of energy transformation and any possible energy savings advantages.

A. Modelled motor

A PMSM of Simscape's Specialized Power Systems sublibrary is used in the model. Mathematical description of the motor follows (1) – (6). The block operates with assumption of linear magnetic circuit with no saturation of stator's and rotor's irons [12]. A three- phased or five- phased machine with sinusoidal back EMF waveform, or a three- phased machine with trapezoidal back EMF can be simulated by this block. Mechanical torque, mechanical angular velocity or mechanical rotational port can be set as input. Type of rotor can also be chosen – round or salient pole.

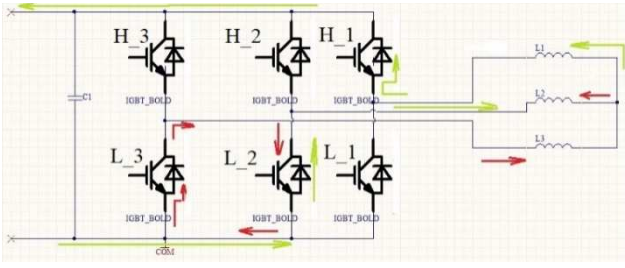


Fig. 2. Short circuit braking strategy

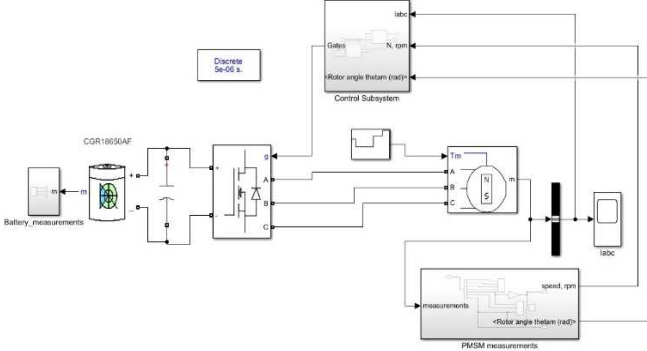


Fig. 3. Simulink model

In the model a three- phased motor with sinusoidal EMF and round rotor (equal d and q inductances) is considered. Mechanical torque (load) is chosen as input. Other electrical and mechanical quantities are set also. These parameters are presented with exemplary values in Table I. Simulation is executed with those values.

B. Modelled battery

Modelling a battery by an equivalent circuit is typically a simple and convenient method of expressing their electrochemical processes. Such equivalent circuits consist of resistors and capacitors, and an open circuit voltage source dependant on state of charge (SoC). Whenever a current is flowing through a battery, there is a difference between terminal voltage V_t and open circuit voltage V_{oc} , known as polarization effect. Transient processes and polarization are represented by groups of RC. Based on number of RC groups models can be categorized as of first order (Thevenin model) or of second order (dual polarization model). Although Thevenin model may present a sufficient simulation of polarization for some applications, polarization is expressed with improved accuracy in dual polarization model [13].

A battery from Specialized Power Systems sublibrary is used in the model [12]. The block allows for a simulation of a lead- acid, a nickel- cadmium, a nickel- metal- hydride or a lithium- ion battery.

Specialized Power Systems' battery block operates with the following limitations and assumptions [12]:

1) Limitations:

- Minimum (no load) voltage is 0 V;
- Maximum voltage is $2E_0$;
- Minimum capacity is 0 Ah;
- Maximum capacity is C_{max} .

2) Assumptions:

- Internal resistance R_0 is assumed to be constant and not variable with current;
- Discharging and charging characteristics are assumed to be the same;

TABLE I. PMSM's parameters exemplary values

| No | Permanent Magnet Synchronous Motor | | |
|----|---|----------------------|-------------------|
| | Parameter and denotation | Value | Units |
| 1 | Stator phase resistance, R | $1.3 \cdot 10^{-2}$ | Ω |
| 2 | Armature inductance, L | $0.75 \cdot 10^{-3}$ | H |
| 3 | Flux linkage by PM, λ | 0.108 | Wb |
| 4 | Number of pole pairs, p/2 | 4 | - |
| 5 | Moment of inertia, J | 10^{-2} | kg.m ² |
| 6 | Viscous damping, F | $5 \cdot 10^{-4}$ | Nm.s |
| 7 | Initial angular velocity, ω_{m0} | 0 | rad/s |
| 8 | Initial angular position, θ_{m0} | 0 | deg |
| 9 | Initial currents, I_A and I_B | 0 | A |

TABLE II. Exemplary values of modelled Li-ion battery's parameters (CGR18650af)

| No | Lithium- ion battery | | |
|----|---|----------------------|------------------|
| | Parameter and denotation | Value | Units |
| 1 | Nominal voltage, V_n | 3.3 | V |
| 2 | Rated capacity, C | 2.05 | Ah |
| 3 | Initial state of charge, SoC ₀ | 30 | % |
| 4 | Maximum capacity, C_{max} | 2.15 | Ah |
| 5 | Cut- off voltage, V_c | 2.15 | V |
| 6 | Fully charged voltage, V_{max} | 4.2 | V |
| 7 | Nominal discharge current, I_D | 1.95 | A |
| 8 | Internal resistance, R_0 | $1.65 \cdot 10^{-2}$ | Ω |
| 9 | Capacity at nominal voltage, C_n | 1.81 | Ah |
| 10 | Exponential voltage, A | 3.71 | V |
| 11 | Exponential capacity, B | 0.6 | Ah ⁻¹ |

c) Lack of Peukert effect (capacity is independent of current);

d) Lack of self discharge. It has to be externally represented;

e) Lack of memory effect.

A Li- ion battery Panasonic CGR18650af is considered [12], [14]. Charge and discharge processes of a Li- ion battery can be expressed by (11) and (12) [1], [12]. Temperature and aging effects are not considered in the model. Simulated parameter's values are given in Table II.

Discharging ($i_{LF} > 0$):

$$E = E_0 - K \frac{C}{C - C_{ext}} i_{LF} - K \frac{C}{C - C_{ext}} C_{ext} + A e^{\frac{-B}{C_{ext}}} \quad (11)$$

Charging ($i_{LF} < 0$):

$$E = E_0 - K \frac{C}{0.1C + C_{ext}} i_{LF} - K \frac{C}{C - C_{ext}} C_{ext} + A e^{\frac{-B}{C_{ext}}} \quad (12)$$

where E is nonlinear voltage in V, E_0 is constant voltage in V, K – polarization constant in V/ Ah, C – maximum capacity in Ah, C_{ext} – extracted capacity (noted as multiplication of battery current and time – i.t) in Ah, i_{LF} – low- frequency current dynamics (of battery current i) in A, A – exponential voltage in V, B – exponential capacity in Ah⁻¹.

Discharge characteristics of Li-ion battery CGR18650af are presented on Fig.4. Two plots are shown on the figure. The top plot presents nominal discharge characteristic with distinctive areas for parameters' values in Table II. On the bottom plot is shown a family of discharge characteristics for various discharge currents.

C. Control subsystem

This subsystem consists of a speed controller and a vector controller. Two types of control algorithms are allowed by vector controller block – SVPWM or hysteresis control. Control subsystem can be seen on Fig. 5. As of this moment only hysteresis type of control has been explored, thus it is the one considered in the model.

D. Simulation

The model is simulated only for 3 seconds and parameters are commonly kept at low values for faster simulation. The input mechanical torque has its amplitude set in such way as to present results in propulsion and braking. Amplitude is varied between 3 Nm for propulsion and -3 Nm for braking. Positive values of input torque operate PMSM as a motor while negative values – as a generator.

At start of simulation, for duration of 0.1 s torque is kept zero as to formally show the off state. At 0.1 s torque is risen to 0.5 Nm for propulsion on flat road. Driving in this way continues for 0.2 s, as at 0.3 s an incline is introduced and torque's value becomes -0.5 Nm. Incline continues for another second. For the duration 1.3 – 1.8 s simulated fictive EV is back on flat road with increased torque input of 0.8 Nm. At 1.8 s for another 0.4 s torque input is further increased to 1.5 Nm. After that at 2.2 s until the end of simulation a negative torque input of -2 Nm is applied as to simulate braking. Input torque's values are presented graphically on Fig. 6.

E. Simulation results

Electromagnetic torque of simulated PMSM is shown on Fig. 7. From the figure it can be seen that it overall follows the shape of input torque (Fig. 6.), but short durations of fluctuations due to inertia are present whenever input torque's value changes.

As hysteresis control is considered in control subsystem, motor's three- phase currents have a hysteresis sinusoidal waveform. This can be seen on Fig. 8. Expected changes in currents' amplitudes and fluctuations in transients according to respective torque's changes are also observed.

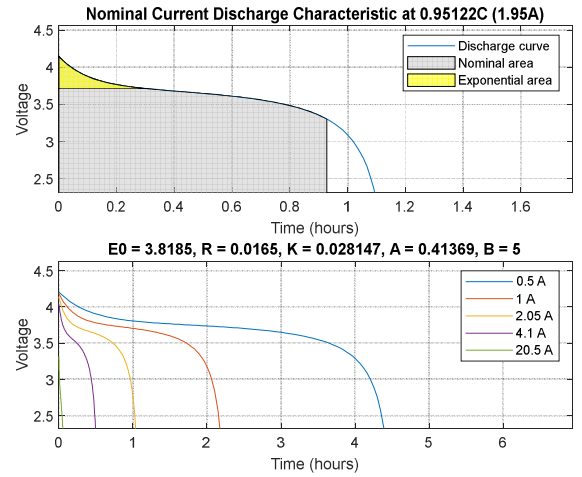


Fig. 4. Discharge characteristics of considered Li-ion battery

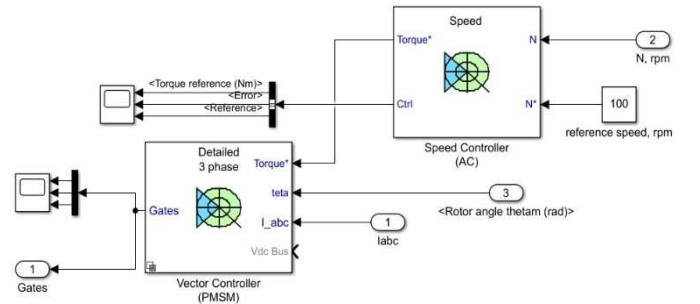


Fig. 5. Control subsystem

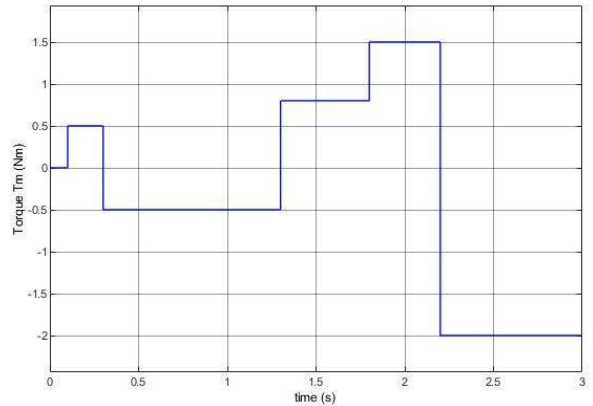


Fig. 6. Input torque reference

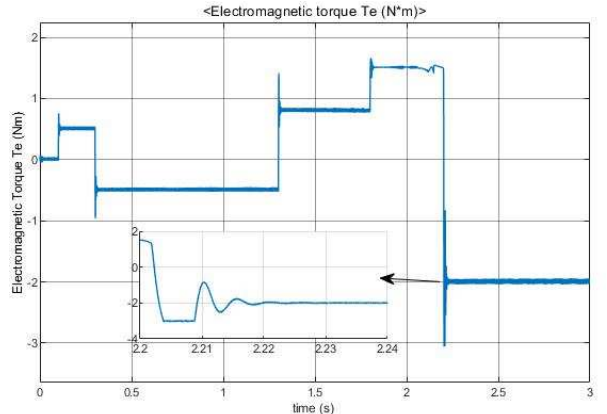


Fig. 7. Electromagnetic torque

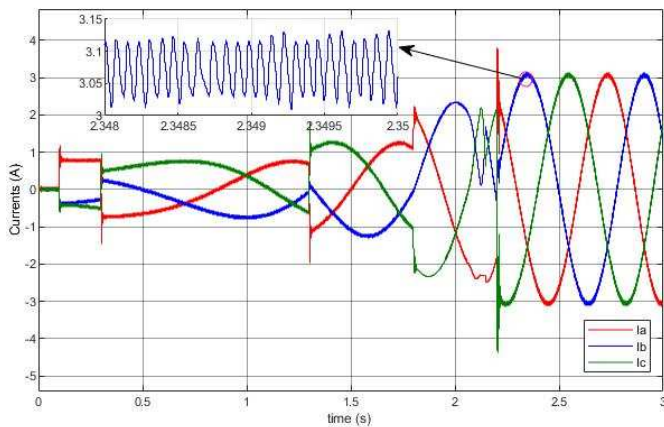


Fig. 8. PMSM's three- phase currents

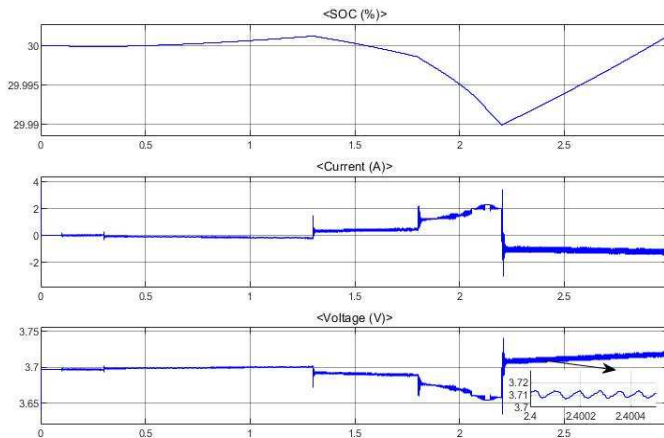


Fig. 9. Battery's SoC, current and voltage

Battery's quantities are shown on Fig. 9. The figure has three plots. First plot shows the relation of battery's State of Charge to time (SoC(t)), while the second and third plots show time relations of battery's current and voltage respectively ($i(t)$ and $V_{batt}(t)$).

During portions of simulation where input torque is negative and PMSM is operated as a generator there are rises in battery's SoC and voltage that can be observed. Current also adopts negative values accordingly as expected for these periods. Thus, it leads to a conclusion that during these portions of time the power converter is operated as a rectifier and battery is being charged.

IV. STUDYING WITH AN EXPERIMENTAL STAND

Physical modelling of a traction system of electric transport by representation of a traction system of electric transport by two coupled motors has been widely applied throughout the years. This representation can also be considered for EV's. One of the motors can be treated as the vehicle's traction motor. The other one can be treated as the load and resistive forces that are experienced during driving.

Physical modelling by an experimental stand allows for a comprehensive and comfortable way of expressing real processes in laboratory environment [15]. A stand to study EV's regenerative braking is being developed. The stand is purposed to produce experimental results which are to be used to verify results obtained from computer simulations. Structure of stand is shown on Fig. 10. The stand is comprised of two coupled three- phase PMSM's, a power converter with control circuit and an energy storage unit. EV's inertia is represented by flywheel mounted between the two motors.

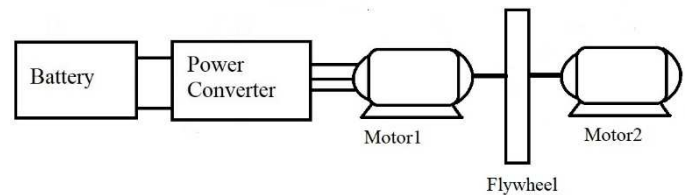


Fig. 10. Concept of stand's structure

During regenerative braking current's direction changes and current's vector has to be in counter- phase to back EMF. Simultaneously, back EMF's vector has to be leading voltage's vector. Back EMF's amplitude also has to be boosted in order to be able to charge the battery [11]. Transition of power converter from inverting to rectifying operation is required. Hence, algorithms and programs to control this transition are of significant importance.

V. CONCLUSIONS

This paper presented a simulation model of an EV's drivetrain system consisting of a battery, a PMSM and a power converter. A hysteresis control has been implemented to control power converter's switches. The following conclusions can be drawn from simulation results – PMSM's currents, although being hysteresis sinusoids, show satisfactory waveforms. Output torque of PMSM is observed that follows the input reference almost identically. Present transients and fluctuations of both currents and electromagnetic torque are of short duration. This is due to inertia. Even though battery's voltage and current waveforms also have hysteresis character, a rise in voltage and SoC during braking periods can be observed, which leads to a conclusion that battery is indeed being charged.

ACKNOWLEDGMENT

The authors would like to thank the Research and Development Sector at the Technical University of Sofia for the financial support.

REFERENCES

- [1] Z. ZARKOV, V. LAZAROV, P. RIZOV, L. STOYANOV and E. POPOV, "An Approach for Modeling the Electronic Converter-Motor System for Electric Vehicles," 2019 16th Conference on Electrical Machines, Drives and Power Systems (ELMA), Varna, Bulgaria, 2019, pp. 1-6, doi: 10.1109/ELMA.2019.8771484.
- [2] A. Joseph Godfrey, V. Sankaranarayanan, A new electric braking system with energy regeneration for a BLDC motor driven electric vehicle, Engineering Science and Technology, an International Journal, Volume 21, Issue 4, 2018, Pages 704-713, ISSN 2215-0986, <https://doi.org/10.1016/j.jestech.2018.05.003>.
- [3] Rafeeq, Farazdaq & Abbas, Roaa. (2018). Design New control System for Brushless DC motor Using SVPWM International Journal of Applied Engineering Research ISSN 0973-4562 Volume 13, Number 1 (2018) pp. 582-589.
- [4] Krishnan, R. (2010). Permanent Magnet Synchronous and Brushless DC Motor Drives. Boca Raton: CRC Press, <https://doi.org/10.1201/9781420014235>
- [5] E. Rachev, V. Petrov and B. Stoev, "Cogging torque effect on motor start-up in a sensorless motor drive for permanent magnet synchronous motors," 2017 15th International Conference on Electrical Machines, Drives and Power Systems (ELMA), Sofia, 2017, pp. 211-214, doi: 10.1109/ELMA.2017.7955434.
- [6] Bozhilov, G. Transient processes and general theory of electric machines. 2007 Technical University – Sofia (Г. Божилов, Преходни процеси и обобщена теория на електрическите машини 2007 Технически Университет – София).
- [7] Grenier, D., L.-A. Dessaint, O. Akhrif, Y. Bonnassieux, and B. LePaiufle. "Experimental Nonlinear Torque Control of a Permanent

- Magnet Synchronous Motor Using Saliency." IEEE® Transactions on Industrial Electronics, Vol. 44, No. 5, October 1997, pp. 680-687.
- [8] T. Rudnicki, R. Czerwinski, D. Polok and A. Sikora, "Performance analysis of a PMSM drive with torque and speed control," 2015 22nd International Conference Mixed Design of Integrated Circuits & Systems (MIXDES), Torun, Poland, 2015, pp. 562-566, doi: 10.1109/MIXDES.2015.7208586.
- [9] Liu, S.-M.; Tu, C.-H.; Lin, C.-L.; Liu, V.-T. Field-Oriented Driving/Braking Control for Electric Vehicles. *Electronics* 2020, 9, 1484. <https://doi.org/10.3390/electronics9091484>
- [10] C., Jarrad & G., Özdemir & N., Zorica & N., Andrew & M., Aaron & H., Odzyskiwanie & Elektrycznych, W. (2009). Regenerative braking in an electric vehicle.
- [11] V. Totev and V. Gueorgiev, "Efficiency of Regenerative Braking in Electric Vehicles," 2020 21st International Symposium on Electrical Apparatus & Technologies (SIELA), Bourgas, Bulgaria, 2020, pp. 1-4, doi: 10.1109/SIELA49118.2020.9167153.
- [12] The Math Works, Inc. (2019). MATLAB (Version 2019b) https://www.mathworks.com/help/physmod/sps/specialized-power-systems.html?s_tid=CRUX_lftnav
- [13] He, Hongwen; Xiong, Rui; Fan, Jinxin. 2011. "Evaluation of Lithium-Ion Battery Equivalent Circuit Models for State of Charge Estimation by an Experimental Approach" *Energies* 4, no. 4: 582-598. <https://doi.org/10.3390/en4040582>
- [14] Panasonic, Lithium Ion Batteries: Individual Datasheet CGR18650AF, January 2007.
- [15] G. Vacheva, R. Stanev and N. Hinov, "Physical model of an electric vehicle for research of dynamic operating modes," 2017 15th International Conference on Electrical Machines, Drives and Power Systems (ELMA), Sofia, 2017, pp. 70-73, doi: 10.1109/ELMA.2017.7955403.